bjh research paper

Angioimmunoblastic T-cell lymphoma: histological progression associates with EBV and HHV6B viral load

Yuanping Zhou,[1] Ayoma D. Attygalle,[2] Shih-Sung Chuang,[3] Tim Diss,[2] Hongtao Ye,[1] Hongxiang Liu,[1] Rifat A. Hamoudi,[1] Philippa Munson,[4] Chris M. Bacon,[1] Ahmet Dogan[5] and Ming-Qing Du[1]

[1]Department of Pathology, University of Cambridge, Cambridge, [2]Department of Histopathology, Royal Marsden Hospital, London, UK, [3]Department of Pathology, Chi-Mei Medical Centre and Taipei Medical University, Taipei, Taiwan, [4]Department of Histopathology, University College London, London, UK, and [5]Divisions of Anatomic Pathology and Hematopathology, Mayo Clinic, Rochester, MN, USA

Received 30 January 2007; accepted for publication 22 March 2007;
Correspondence: Prof. Ming-Qing Du, Department of Pathology, Division of Molecular Histopathology, University of Cambridge, Box 231, Level 3, Lab Block, Addenbrooke's Hospital, Hills Road, Cambridge CB2 2QQ, UK. E-mail: mqd20@cam.ac.uk

Summary

The clinical and histological presentations of angioimmunoblastic T-cell lymphoma (AITL) often mimic an infectious process. Epstein–Barr virus (EBV) and human herpes virus (HHV6) are known to be associated with AITL, but whether these viral infections play a role in its pathogenesis is unclear. It also remains to be investigated whether there might be other viruses associated with AITL. We first screened 26 well-characterised cases of AITL for herpesvirus by polymerase chain reaction (PCR) with universal primers and found evidence of only EBV and HHV6B infection. Subsequent PCR using virus-specific primers demonstrated EBV and HHV6B infection in 40/49 biopsies (36/42 cases) and 21/49 biopsies (19/42 cases) of AITL respectively with both viral infections found in 17/49 specimens (15/42 cases). Importantly, simultaneous infection with both viruses was found only in specimens showing histological pattern II ($n = 2$) or III ($n = 15$). Interestingly, among specimens containing both viruses, there was a tendency towards an inverse correlation between the EBV and HHV6B viral load as shown by quantitative PCR. In specimens positive only for EBV, the viral load was significantly higher in specimens with histological pattern III than those with pattern II. High EBV load was also significantly associated with B-cell monoclonality. Double EBV encoded small RNA (EBER) *in situ* hybridisation and immunohistochemistry indicated that EBV-infected B cells had a late postgerminal centre immunophenotype. Our results demonstrate an association between EBV and HHV6B infection and the histological progression of AITL, suggesting that these viruses may play a role in the pathogenesis of this lymphoma.

Keywords: angioimmunoblastic T-cell lymphoma, histological progression, Epstein–Barr virus, HHV6B.

Angioimmunoblastic T-cell lymphoma (AITL) is a neoplasm of mature T cells which occurs mostly in the middle-aged and elderly (Dogan *et al*, 2003). Patients typically present with a systemic illness, characterised by B-symptoms (such as fever and night sweats), generalised lymphadenopathy, and often hepatosplenomegaly and a skin rash, in many cases mimicking an infectious process (Dogan *et al*, 2003). Abnormal haematological and immunological laboratory indices are frequent and many patients exhibit autoimmune phenomena and immune dysfunction (Dogan *et al*, 2003). Histologically, the lymphoma is characterised by partial or complete effacement of the normal lymph node architecture by a polymorphic lymphoid infiltrate including neoplastic T-cells that are often CD10 positive, various chronic inflammatory cells, prominent high endothelial venules and expanded follicular dendritic cell (FDC) networks (Attygalle *et al*, 2002).

The histological architecture of AITL may be classified into three overlapping patterns (Attygalle *et al*, 2002). In pattern I, the lymph node architecture is largely preserved. Hyperplastic B-cell follicles are surrounded by an expanded paracortex containing a polymorphic infiltrate of lymphocytes, transformed large lymphoid blasts, plasma cells, macrophages and

© 2007 The Authors

eosinophils within a prominent vascular network. FDC show little or no evidence of expansion outside of the follicles. Pattern II is characterised by loss of the normal lymph node structure, except for the presence of occasional regressed/depleted follicles. On immunostaining, these cases show FDC proliferation beyond the follicles. The remainder of the node shows a polymorphous infiltrate and vascular proliferation similar to that of pattern I. In pattern III, the normal lymph node structure is completely effaced, with prominent irregular and perivascular proliferation of FDCs, extensive vascular proliferation and a diffuse polymorphic infiltrate similar to that seen in patterns I and II. These morphological patterns are associated with increasing numbers of neoplastic CD10-positive T cells, which spread from an intra- or peri-follicular location in pattern I to a more diffuse distribution in patterns II and III. In several patients in whom sequential biopsies have been examined, we and others have observed a transition from pattern I histology to pattern III histology over time (Ree *et al*, 1998; Attygalle *et al*, 2002; Attygalle *et al*, 2007a). Thus, these histological patterns appear both to reflect quantitative differences in the number of neoplastic cells present and to represent temporal progression of disease.

Infectious agents, both directly oncogenic [e.g. Epstein–Barr Virus (EBV) in classical Hodgkin lymphoma] and co-stimulatory [e.g. *Helicobacter pylori* in gastric mucosa-associated lymphoid tissue (MALT) lymphoma] have been associated with numerous lymphoproliferative disorders (Wotherspoon, 1997; Kuppers, 2003). Both the clinical presentation and polymorphic histological appearances of AITL raise the possibility of a role for infectious agents in its pathogenesis. Several infectious agents including EBV, human herpesvirus (HHV) 6, HHV8 and hepatitis C virus have been reported to be associated with AITL. Among them, EBV, HHV6 and HHV8 appear to be most relevant as they are not only lymphotropic but also oncogenic. EBV is found in most cases of AITL as shown by EBV encoded small RNA (EBER) *in situ* hybridisation (ISH) (Weiss *et al*, 1992; Khan *et al*, 1993; Attygalle *et al*, 2007b), while HHV6 was reported in 22–58% cases of AITL by polymerase chain reaction (PCR) (Luppi *et al*, 1993; Vrsalovic *et al*, 2004). However, neither EBV nor HHV6 is found in the neoplastic T-cells themselves, suggesting a lack of a direct cell autonomous role in lymphomagenesis. HHV8 was detected in occasional cases of AITL by PCR in a single study (Luppi *et al*, 1996), but subsequent studies failed to show any evidence of HHV8 involvement in AITL by both PCR and immunohistochemistry (Chadburn *et al*, 1997). Nonetheless, it remains to be determined whether infectious agents play a role in the pathogenesis of AITL, perhaps by inducing microenvironmental conditions which promote lymphoma progression, even if not playing a direct initiating role. It also remains to be investigated whether there are other viruses, which might be associated with the development of AITL.

In view of the pivotal role of several types of herpesvirus in a number of lymphoproliferative disorders, we screened a series of well-characterised AITL cases for herpesvirus by PCR with universal primers and found evidence of only EBV and HHV6B infection. To understand the role of EBV and HHV6B infection in the pathogenesis of AITL further, we determined the cell type carrying EBV, measured the EBV and HHV6B viral load in lymphoma tissues by quantitative real-time PCR and correlated the viral load with histological progression.

Materials and methods

Materials

Formalin-fixed and paraffin-embedded tissue (49 specimens) and frozen tissue (5) from 42 cases of AITL histologically and immunophenotypically characterised as described previously were retrieved from the authors' institutions (Attygalle *et al*, 2002). The use of redundant archival tissues for research was approved by the local research Ethics Committees of the authors' institutions.

DNA extraction

De-waxed formalin-fixed paraffin-embedded tissue sections and frozen tissue sections were digested with proteinase K (2 mg/ml) in 30 mmol/l Tris–HCl (pH 8.0) buffer containing 10 mmol/l EDTA and 1% sodium dodecyl sulphate at 55°C for 2 d. DNA was extracted by using the Wizard genomic DNA purification kit (Promega, Southampton, UK). High molecular weight DNA was extracted from normal peripheral blood leucocytes and the Burkitt lymphoma cell line Namalwa (diploid and carries two copies of EBV genome/cell) using QIAGEN DNA extraction kits (QIAGEN, West Sussex, UK), and they were used for preparation of the standard curve for quantification of EBV load using real time PCR. DNA was quantified by using GeneQuant pro (Amersham pharmacia biotech, Cambridge, UK).

Identification of human herpesvirus in AITL samples by PCR

To identify possible, potentially novel, human herpesvirus infection in AITL, we first screened the lymphoma specimens using PCR with universal primer pairs, which targeted a well-conserved region of the DNA polymerase gene of known human herpesviruses. The universal primer pair 1 (HU1-s and HU1-as) targeted herpes simplex virus type-1 (HSV-1), HSV-2, cytomegalovirus (CMV), EBV and HHV8, while the universal primer pair 2 (HU2-s and HU2-as) amplified HHV6 (variant A and B), Varicella-zoster virus (VZV) and HHV7 (Table I). PCR conditions for these primer pairs were optimised with known positive controls and then applied to DNA extracted from AITL tissue specimens. The PCR cycling parameters with the HU1 primer pair were: 95°C × 5 min, followed by 5 touch down cycles of 95°C × 1 min, 60–56°C (reduce 1°C each cycle) × 1 min, 72°C × 1 min, then 35 cycles of 94°C × 45 s, 55°C × 1 min, 72°C × 1 min, and a final extension of 7 min

© 2007 The Authors
Journal Compilation © 2007 Blackwell Publishing Ltd,

Table I. Polymerase chain reaction (PCR) primers used for screening herpesviruses.

Primer name	Gene target	Sequence	Amplicon size
Consensus primer sets for herpesviruses			
HU1-s1	Herpesvirus DNA polymerase	GTGGTGGACTTTGCCAGCCTGTACCC	herpes simplex virus type-1 (HSV-1) (532) HSV-2 (532) Epstein–Barr virus (EBV) (538)
HU1-as1		TAAACATGGAGTCCGTGTCGCCGTAGATGA	Cytomegalovirus (604) human herpes virus (HHV8) (526)
HU2-s1	Herpesvirus DNA polymerase	GTCGTGTTTGATTTTCAAAGTTTATATCC	VZV (536) HHV6 (533)
HU2-as1		ATAAACACACAATCCGTATCACCATAAATAACCT	HHV7 (533)
Specific primer sets for EBV and HHV6			
EBV-EBNA-s1	EBV EBNA	GGACCTCAAAGAAGAGGGGG	80 bp
EBV-EBNA-as1		GCTCCTGGTCTTCCGCCTCC	
U11-S2	HHV6 U11 open	AATCTAAAATCCCCGAAGGGC	HHV6B (111 bp)
U11-AS2	reading frame	TCTCTTTAATGTCCGGAGTTGA	HHV6A (147 bp)
Primer sets for real time PCR			
EBNA106-s	EBV EBNA	CCGGTGTGTTCGTATATGGAG	106 bp
EBNA106-as		GGGAGACGACTCAATGGTGTA	
HHV6 Pol-96s	HHV6 Pol-96S	GCACAGCATAATAACCCGTCTTAG	96 bp
HHV6 Pol-96as		TGATTCTTCCGAGTATGGTGTCTTC	
β2M-s	human β-2 microglobulin	TGCTGTCTCCATGTTTGATGTATCT	86 bp
β2M-as		TCTCTGCTCCCCACCTCTAAGT	

at 72°C. With the HU2 primer pair, the PCR cycling parameters were: 95°C × 5 min, followed by 40 cycles of 94°C × 1 min, 47°C ×1 min, 72°C × 1 min, and a final extension at 72°C for 7 min. PCR products were analysed on 8% polyacrylamide gels. Amplified products were sequenced in both orientations using dRhodamine dye terminators on an ABI Prism 377 sequencer (PE Applied Biosystems, Foster City, CA, USA) to identify the type of herpesvirus.

For EBV and HHV6 screening, primers were designed to flank a short (80–147 bp) fragment, so as to be suitable for amplification of DNA extracted from archival paraffin-embedded tissues. The primers for EBV targeted Epstein–Barr nuclear antigen-1 (EBNA-1), while those for HHV6 amplified the HHV6 U11 open reading frame (ORF), yielding different-sized products between HHV6A and HHV6B (Table I). PCR conditions were optimised by using known positive and negative controls. The PCR cycling parameters for the EBNA-1 and HHV6 U11 primer pairs were: 95°C × 5 min, followed by 10 touch down cycles of 94°C × 45 s, 60–56°C (reduce 1°C every 2 cycles) × 1 min, and 72°C × 1 min; then 30 cycles of 94°C × 45 s, 55°C × 1 min, 72°C × 1 min, and finally 72°C for 7 min. The PCR products were analysed on 10% polyacrylamide gels.

Quantification of EBV and HHV6 load in tumour tissue

This was carried out by quantitative real-time PCR (qPCR) using an iCycler iQ system (BIO-RAD, Hemel Hempstead, UK) with SYBR Green I. Human β-2 microglobulin (β2 M) was used as an internal control. The primers for EBV targeted EBNA-1, while those for HHV6 amplified a short region of the viral DNA polymerase (Table I). All the primer pairs were designed to flank a short fragment and were thus suitable for archival-fixed tissues. The conditions for real-time PCR were systematically optimised prior to data collection. Briefly, the specificity of the PCR products for each primer set was confirmed by melt-curve analysis and by electrophoresis on 10% polyacrylamide gels.

The standard curves were generated by serial dilutions of EBV-positive DNA extracted from Namalwa cells or the pRPMS4.4 plasmid containing the HHV6 DNA polymerase gene into high molecular DNA from normal peripheral blood leucocytes. The average coefficient value (R^2) for each of the three standard curves was above 0·99 and the relative efficiency of amplification of EBV and HHV6 was close to that of β2 M as the absolute value of the slope of log input amount of DNA vs. ΔC_T, the difference of threshold cycle numbers between β2 M and each of EBV and HHV6, was below 0·1.

Following the optimisation of the experimental conditions, real-time PCR was performed separately in a 25-μl reaction mixture containing 12·5-μl SYBR Green Super-Mix (BIO-RAD), 200 nmol/l of each sense and anti-sense primer, and 200 ng template DNA. All samples were amplified in triplicate in a 96-well plate by 40 cycles of denaturation at 95°C for 3 min and annealing and extension at 60°C for 1 min. Real-time PCR of β2 M was run in parallel for each sample. Melt-curve analysis was performed immediately after the amplification protocol for each case and only samples that showed specific amplification were included in the data

© 2007 The Authors

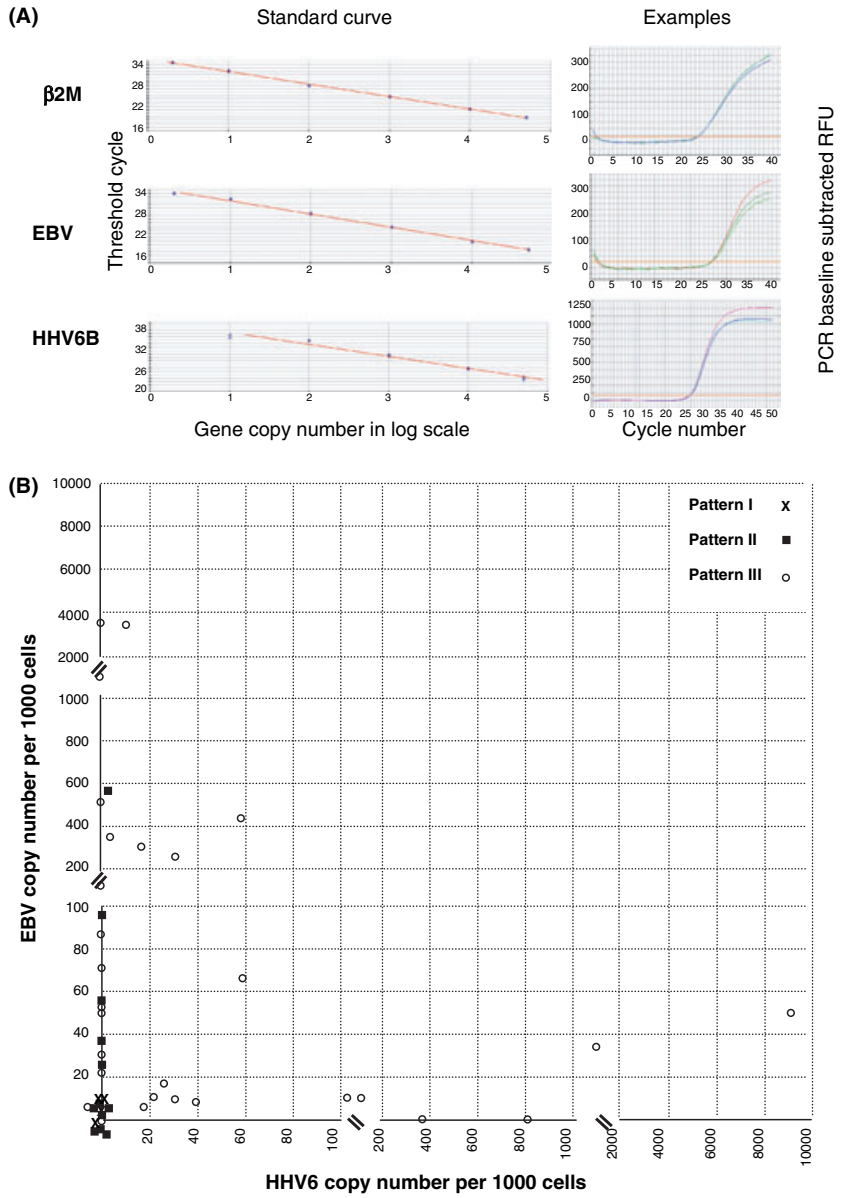

Fig 1. Epstein–Barr virus (EBV) and human herpes virus (HHV6) viral load in angioimmunoblastic T-cell lymphoma (AITL). (A) Standard curves (left panel) and examples (right panel) of real-time polymerase chain reaction for quantification of EBV and HHV6B viral loads in tissue specimens involved by AITL. (B) Correlation between histological pattern and EBV and HHV6 viral load in tumor tissues.

analysis. The virus copy number per 1000 cells was calculated after obtaining virus copies and β2 M copies according to the related ΔC_T values and the standard curves respectively as described above. Under the above conditions, it was possible to reliably quantify EBV and HHV6 copy numbers as low as 5 and 10 per 1000 cells, respectively (Fig 1A).

B- and T-cell clonality analysis

These were performed by PCR analyses of the rearranged immunoglobulin genes and T-cell antigen receptor (TCR) genes using Fr3-JH PCR and TCRγ PCR respectively as described previously (Diss *et al*, 1993; Diss *et al*, 1995).

EBER-ISH

This was carried out with a PCR-generated DNA probe labelled with digoxigenin, followed by incubation with anti-digoxigenin-AP and visualisation with 5-bromo-4-chloro-3-indolyl phosphate and 4-nitro blue tetrazolium chloride (Boehringer Ingelheim, Ingelheim, Germany) (Pan *et al*, 1995).

Immunohistochemistry

Paraffin-embedded tissue sections were immunostained by using the streptavidin immunoperoxidase method (ChemMate

© 2007 The Authors
Journal Compilation © 2007 Blackwell Publishing Ltd,

Streptavidin Peroxidase kit, DakoCytomation, Cambridge, UK) and DAB chromogen (DakoCytomation) following heat-mediated antigen retrieval (Attygalle *et al*, 2002). Primary antibodies included CD3 (DakoCytomation, polyclonal), CD20 (DakoCytomation, L26), CD79a (DakoCytomation, JCB117), CD10 (Novocastra, Newcastle upon Tyne, UK, 56C6), Bcl-6 (DakoCytomation, M7211), MUM-1/IRF-4 (DakoCytomation, MUM1p) and CD138 (Novocastra, 5G10), kappa (DakoCytomation, polyclonal anti-kappa) and lambda (DakoCytomation, polyclonal anti-lambda). Sequential double-layered immunohistochemistry and EBER-ISH for CD3/EBER, CD10/EBER, CD20/EBER and CD79a/EBER was carried out on selected cases as follows: EBER-ISH was performed as described above (without counterstaining) and the sections were then subjected to immunohistochemistry performed as described above, except that the primary antibody was applied for 3 h.

Statistical analysis

Chi-squared and Fisher's exact test were used to analyse the correlation between EBV and HHV6B viral load and either different histological patterns or B- and T-cell clonality. Pearson's regression analysis was used to examine the correlation between EBV and HHV6B viral loads.

Results

Incidence of EBV and HHV6 infection in AITL

To identify the possible, potentially novel, human herpesvirus infection in AITL, we first screened 26 cases of AITL, including five with high molecular weight DNA from frozen lymphoma tissues, using PCR with universal primer pairs against herpesvirus DNA polymerase. Nine cases showed a positive PCR product with universal primer set 1 (HU1): three cases with high molecular weight DNA and six cases with DNA from the fixed tissue only. Three cases, all of which also showed a positive PCR product with primer set HU1, displayed a positive PCR product with universal primer set 2 (HU2). Sequencing analysis revealed that the 9 PCR products obtained using the HU1 primer set belonged to EBV, while the 3 PCR products obtained using the HU2 primer set were from HHV6B.

As the fragments targeted by the universal PCR primer sets were relatively long (between 532 and 604 bp), it was highly possible that this protocol might not identify EBV or HHV6 in all fixed tissue samples. To investigate the true incidence of EBV and HHV6 infection in AITL, we therefore performed PCR screening using primer sets specifically designed for application to archival fixed tissues. The primers for HHV6 were designed to amplify both HHV6A and HHV6B, but with different-sized amplicons, such that the two subtypes were readily distinguishable on polyacrylamide gels. The quality of extracted DNA was assessed by PCR of variously sized fragments of the G6PD gene and only samples with adequate DNA integrity were used for viral screening. EBV DNA was found in 40 of 49 biopsies (36/42 cases). Thirty-nine of these biopsies showed features of AITL alone while one biopsy showed features of AITL- and EBV-associated diffuse large B-cell lymphoma (DLBCL). HHV6 DNA was identified in 21/49 biopsies (19/42 cases) evaluated, with all HHV6 positive biopsies containing HHV6B. Of these positive biopsies, 17 specimens (15/42 cases) were positive for both EBV and HHV6B.

Correlation of EBV and HHV6B viral load with histological progression

Quantification of EBV and HHV6B viral load by qPCR was successfully performed in a total of 45 specimens from 42 cases of AITL, in which the histological pattern was determined. Of these 45 specimens, four showed pattern I histology, 12 displayed pattern II and 29 showed pattern III.

HHV6B infection was found exclusively in specimens with histological patterns II or III, and was present in significantly more cases with pattern III histology (17/29 = 58·6%) than those with pattern II histology (2/12 = 16·7%) ($P < 0·014$) (Table II). Moreover, amongst the HHV6B-positive cases, the HHV6B viral load was dramatically higher in cases with pattern III histology (median = 40 copies/1000 cells) than those with pattern II (median = 0·7 copies/1000 cells) (Fig 1B).

In contrast to HHV6B, there was no statistically significant difference in the incidence of EBV infection among specimens with different histological patterns (Table II). However, amongst the EBV-positive cases, the EBV load was much higher in cases with histological patterns II and III (median = 34 copies/1000 cells) than in those with pattern I (median = 8 copies/1000 cells) (Fig 1B) although this did not reach the statistical significance, most likely because of the small number of cases with pattern I histology. Interestingly, in two cases in which sequential biopsies showed progression from pattern I to pattern III, there was a dramatic increase in the EBV load in the second biopsy (0 copies/1000 cells in pattern I and 1124 copies/1000 cells in pattern III in one case,

Table II. Correlation of histological patterns of angioimmunoblastic T-cell lymphoma with Epstein–Barr virus (EBV) and human herpes virus (HHV6) infection*.

	Histological pattern		
	Pattern I	Pattern II	Pattern III
EBV +ve, HHV6B +ve	0	2	15
EBV +ve, HHV6B −ve	3	7	11
EBV −ve, HHV6B +ve	0	0	2
EBV −ve, HHV6B −ve	1	3	1
No of specimens	4	12	29

*Only specimens with qPCR data for the EBV and HHV6 viral load are included.

© 2007 The Authors

15 copies/1000 cells in pattern I and 56 copies/1000 cells in pattern II in the other). In contrast, in two other cases in which sequential biopsies each showed pattern III histology, there was no increase in EBV load in the second biopsy.

Seventeen specimens were positive for both EBV and HHV6B. Fifteen of these specimens showed pattern III histology and the remaining two cases displayed pattern II. Interestingly, among the samples positive for both viruses, there was a trend that the EBV load inversely correlated with the HHV6B load, such that the samples with the highest EBV or HHV6B loads had relatively low levels of the other virus. However, this trend did not reach statistical significance (Fig 1B). In two cases initially treated by CHOP (cyclophosphamide, doxorubicin, vincristine, and prednisone) where material was available from a follow-up biopsy showing no change in histological pattern, the inverse relationship between EBV and HHV6B loads seen in the diagnostic biopsy was maintained in the follow-up biopsy in at least one case (15 EBV copies/1000 cells and 104 HHV6B copies/1000 cells in the diagnostic biopsy, and 35 EBV copies/1000 cells and 1534 HHV6B copies/1000 cells in the follow-up biopsy in one case; 418 EBV copies/1000 cells and 59 HHV6B copies/1000 cells in the diagnostic biopsy, and 65 EBV copies/1000 cells and 59 HHV6B copies/1000 cells in the follow up biopsy in the other). In view of the above finding of an inverse correlation between EBV and HHV6B loads, we further compared the EBV load between HHV6B negative cases showing either patterns II or III. The results revealed a significant difference between the two subgroups, with much higher EBV load in cases with pattern III (mean = 64 copies/1000 cells) than in those with pattern II (8 copies/1000 cells) ($P < 0{\cdot}05$). All pattern I cases were HHV6B negative, with very low or undetectable levels of EBV. Interestingly, among these HHV6B negative cases, four cases (three with histological pattern III and 1 with histological pattern II) showed high levels of EBV loads (500–3697 copies/1000 cells), consistent with the above observation that high EBV and HHV6B loads were mutually exclusive.

We also correlated EBV and HHV6B viral loads with B- and T-cell clonality. Of the 45 specimens examined, nine showed a monoclonal pattern with IGH Fr3-JH PCR, indicating presence of a clonal B-cell population. Each of these nine samples contained EBV as demonstrated by PCR and/or ISH. The incidence of B-cell monoclonality was significantly higher in cases (4/9 = 44%) with a high EBV load (≥200 copies/1000 cells) than in those (5/36 = 14%) with a low viral load (<200 copies/1000 cells) ($P < 0{\cdot}05$). One of the cases with high EBV load had developed an EBV-associated DLBCL while another case subsequently developed an EBV-associated classical Hodgkin lymphoma. Unlike EBV, there was no association between HHV6B viral load and B-cell clonality. In addition, there was no correlation between EBV or HHV6B viral load and T-cell clonality.

Nature of the EBV-infected cells in AITL

To determine the nature of the EBV-positive cells in AITL, double-layered immunohistochemistry (CD3, CD20, CD79a, CD10) and EBER-ISH was performed in four selected samples. EBER/CD20 showed that although some EBER positive cells were CD20 positive B cells, there were many EBV-infected cells that were CD20 negative (Fig 2A). In contrast, staining for CD79a, which is present on B cells including those showing plasmacytoid differentiation, highlighted all EBER positive cells (Fig 2B). All the EBER-positive cells were negative for the germinal centre marker CD10, and were distinct from the CD10 positive neoplastic T-cells (Fig 2C).

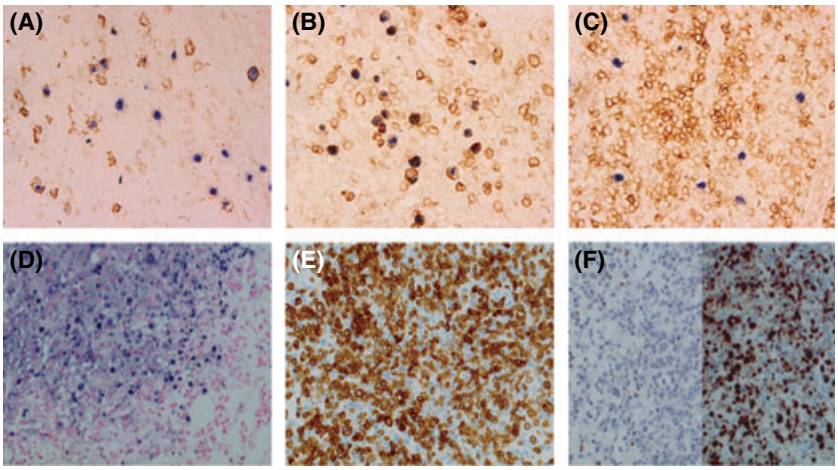

Fig 2. Immunophenotypic characteristics of Epstein–Barr virus (EBV)-positive B-cells in angioimmunoblastic T-cell lymphoma. Double-layered EBV-encoded small RNA (EBER)-ISH (blue) and immunohistochemistry (brown) shows that only some of the EBER-positive cells express CD20 (A), while all EBER-positive cells express CD79a (B). Double EBER-ISH and CD10 staining shows that the CD10-positive neoplastic population is distinct from the EBER-positive cells (C). EBER-ISH shows diffuse EBER-positive cells of a diffuse large B-cell lymphoma in a case of AITL (D). Immunostaining of consecutive sections show that EBER-positive cells express. CD79a (E) and MUM-1/IRF4 (F, right panel), but not Bcl6 (F left panel).

© 2007 The Authors
Journal Compilation © 2007 Blackwell Publishing Ltd,

To further characterise the immunophenotype of the EBV-positive cells, we investigated a follow-up specimen in a case of AITL that contained sheets of EBV-positive B cells (EBV-associated DLBCL). Consecutive sections were used for EBER-ISH and single layered immunohistochemistry. The additional immunohistochemistry showed that the EBER positive B-cells were MUM-1/IR4 positive but negative for the germinal centre marker Bcl-6 (Fig D–F) and negative for the mature plasma cell marker CD138. Light chain staining showed abundant cytoplasmic Ig and kappa light chain restriction in the EBV-positive B-cell population. Together, these findings suggest that the EBV-infected B-cells in AITL show an immunoblastic/plasmablastic immunophenotype.

Discussion

By PCR screening with universal primers targeting known herpesviruses, we found evidence of EBV and HHV6B, but not other herpesviruses, in AITL. Association of HHV6B and EBV with AITL has been previously reported (Weiss *et al*, 1992; Khan *et al*, 1993; Luppi *et al*, 1993; Vrsalovic *et al*, 2004; Attygalle *et al*, 2007b). We have now extended the previous observations, finding HHV6B in nearly half of a large series of AITL and EBV in almost all of our cases, and further showed that EBV was present in B cells that exhibit immunohistochemical features of postgerminal centre differentiation. More importantly, we have also revealed a clear association between histological progression and the load (copy number) of both EBV and HHV6B in the lesional tissue. These findings suggest a dynamic interplay between HHV6B and EBV and the progression of AITL and raise the following possibilities: (1) EBV and HHV6B infection may play an active role in the pathogenesis of AITL and may be, at least in part, responsible for the histological progression and clinical features of the disease; (2) the increased EBV and HHV6B viral load during histological progression of AITL may be a consequence of increasing dysfunction of the immune system during lymphoma progression, the viruses being passengers during the disease process; and (3) a combination of both the above possibilities exists.

The importance of EBV as a pathogen in immunocompromised people is well recognised. More recently, it has also been shown that reactivation of HHV6 from latency occurs in immunocompromised states such as post-transplant immunosuppression, and is associated with recognisable clinical syndromes (Wang *et al*, 2006). Many patients with AITL have features of immunodeficiency, which appears to be a consequence of the tumour itself rather than a pre-existing condition, and is characterised by a reduction in circulating T cells, an inverted CD4/CD8 ratio and defective T-cell function *in vivo* and *in vitro* (Pizzolo *et al*, 1983; Ganesan *et al*, 1987). This underlying immune dysfunction may well provide the background for infection with, or reactivation of, EBV and/or HHV6 in patients with AITL.

There are several pieces of evidence to suggest that this viral infection may then play an active role in the progression of AITL. In particular, it is significant that the neoplastic T cells in AITL only account for a small proportion, typically 5–30%, of the total cell population in a lymph node (Attygalle *et al*, 2002; Willenbrock *et al*, 2005), while the majority of cells are a polymorphous paracortical mix of reactive, often immunoblastic, B and T cells, plasma cells, macrophages and eosinophils within a prominent vascular network. A somewhat similar paracortical expansion by polymorphic lymphoid cells may be seen in non-neoplastic viral lymphadenitis caused by members of the herpesvirus family, including EBV and HHV6 (Schnitzer, 1995; Maric *et al*, 2004). It is possible that both EBV and HHV6 may play an important role in the development of the tumour microenvironment of AITL. This situation is analogous to that of classical Hodgkin lymphoma, in which scattered neoplastic Hodgkin/Reed-Sternberg (HRS) cells interact with a prominent inflammatory infiltrate to orchestrate tumour formation. Aside from directly promoting the proliferation and survival of HRS cells (Kuppers, 2003), EBV is also thought to modify the function of these infiltrating inflammatory cells (Dukers *et al*, 2000; Skinnider & Mak, 2002). Interestingly, HHV6 has also been identified in almost one-third of Hodgkin lymphomas (Di Luca *et al*, 1994), and may play a similar modulatory role. The significant association between EBV and HHV6 viral load and histological progression of AITL may therefore signify a reciprocal causal relationship: on the one hand, EBV and HHV6 could promote recruitment of the inflammatory infiltrate, which contributes to disruption of the normal lymphoid structure and the histological progression of AITL, while on the other hand, destruction of normal lymphoid tissues could promote further deterioration of immune function, thus exacerbating the viral infection. In this regard, it is noteworthy that the highest loads of EBV and HHV6 detected by quantitative RT-PCR were mutually exclusive. If these viruses are simply inactive passengers during the disease process one would expect to see high levels of both viral loads in at least some of the pattern III cases.

Previous studies of EBV, HHV6 and lymphoma suggest several ways in which these viruses might promote the progression of AITL. Most notably, each virus both contains genes encoding viral homologues of human cytokines, chemokines and their receptors, and modulates the production of cytokines, chemokines and receptors by lymphocytes and inflammatory cells. For example, HHV6 contains a chemokine gene U83, and chemokine receptor genes such as U12 (Isegawa *et al*, 1998; Zou *et al*, 1999). Similarly, the EBV genome contains BCRF1, a homologue of IL-10 (Moore *et al*, 1990). Several studies have shown that both HHV6 and EBV can modulate the production of, and response to, cytokines and chemokines such as IL-1, IL-2, IL-6, IL-10, IL-12, IL-15, IL-18, IFNγ, TNFα and CCL5 (RANTES) by many cell types (Gosselin *et al*, 1992; Flamand *et al*, 1995; Klein *et al*, 1996; Arena *et al*, 1999; Arena *et al*, 2001; Uchihara *et al*, 2005). Thus, it can be proposed that by modulating the cytokine

© 2007 The Authors

milieu, EBV and HHV6 might promote the acquisition of the polymorphous infiltrate seen in AITL, contributing to disease progression. Moreover, the ability of many of the cytokines discussed above to promote the survival and proliferation of T cells suggests that EBV and HHV6 might also indirectly promote the expansion of the neoplastic T cells in AITL. Again, this situation is analogous to that seen in classical Hodgkin lymphoma, in which cytokines and chemokines such as IL-13, TARC, eotaxin, IL-10 and TGFβ are thought to be responsible for HRS cell survival, recruitment of T cells and eosinophils, suppression of cytotoxic T-lymphocyte function and fibrosis, respectively (Skinnider & Mak, 2002).

In addition to the above, at least two other mechanisms by which EBV and HHV6 might promote progression of AITL are suggested by our knowledge of the biology of the viruses and of AITL itself. Firstly, *in vitro* and *in vivo* data show that HHV6 is able to induce depletion and functional suppression of T lymphocytes (Flamand *et al*, 1995; Yasukawa *et al*, 1998; Gobbi *et al*, 1999). Together with the liberation of anti-inflammatory cytokines such as IL-10, it is possible that such effects could contribute to the immunosuppression seen in AITL. Secondly, the perifollicular localisation and expression of CD10, Bcl-6 and CXCL13 by the neoplastic T cells in AITL suggests that the tumour may originate from follicle centre T cells (Ree *et al*, 1999; Attygalle *et al*, 2002; Grogg *et al*, 2005). The survival and proliferation of these T cells is regulated by interactions with FDC, and indeed FDC expansion is a key feature of AITL. It is therefore intriguing that Luppi *et al* (1998) identified HHV6 by immunohistochemistry in FDC in cases of Rosai–Dorfman disease. Although we have not been able to verify the specificity of the available anti-HHV6 antibodies, and have therefore not been able to identify which cells harbour HHV6 in our cases, the results of Luppi *et al* at least raise the possibility that HHV6 might modulate the neoplastic T cells in AITL by affecting the tumour-associated FDC. The principle that an infectious agent may play a central role in lymphomagenesis without being present in the lymphoma cells themselves is now well established. For example, in gastric MALT lymphoma, the growth of tumour B-cells depends critically upon a T-cell-mediated immune response to *H. pylori* rather than direct stimulation by the bacterium (Hussell *et al*, 1996). As discussed above, similar indirect mechanisms may apply to the role of EBV and HHV6 in AITL.

There is also clinical evidence to suggest a role for EBV and/or HHV6 in the clinicopathological presentation and outcome of AITL. Battegay *et al* (2004) reported a case of AITL that showed complete remission following treatment with the antiviral agent valacyclovir alone. They demonstrated that the occurrence and size of enlarged lymph nodes, as well as systemic symptoms such as fatigue and night sweats, were strongly correlated with the EBV load in peripheral blood. Recently, Strupp *et al* (2002) and Dogan *et al* (2005) reported impressive treatment responses of AITL to thalidomide, an anti-angiogenic and anti-inflammatory drug. Significantly, Dogan *et al* (2005) showed thalidomide treatment was associated with the disappearance of EBV positive cells. This was accompanied by a reduction in the extent of the polymorphic infiltrate and by alteration of the vascular architecture. There was a marked reduction in the number of CD10 positive neoplastic T cells in the perifollicular areas, and those that remained occupied the centres of regressed follicles with reduced FDC meshworks. These clinical reports thus suggest that reduction of EBV load in AITL may be of clear clinical benefit. It is also intriguing that many of the clinical features of AITL are similar to those induced by HHV6 reactivation in immunocompromised hosts, including skin rash, arthritis and bone marrow suppression. However, whether HHV6 plays a role in the systemic clinical features of AITL remains a matter of speculation.

In this study, we have demonstrated an association among EBV, HHV6B and the histological progression of AITL, raising the possibility that these viruses may play a role in the pathogenesis of this lymphoma. The present work forms a platform for further studies investigating both the biological mechanisms of such a role and the clinical importance of HHV6B and EBV load in the course and management of AITL patients, and provides a further avenue for understanding this enigmatic disease.

Acknowledgements

This study was supported by research grants from the Association of International Cancer Research and Leukaemia Research Fund, UK. Chris Bacon is supported by a Senior Clinician Scientist Fellowship from The Health Foundation, The Royal College of Pathologists and The Pathological Society of Great Britain and Ireland. We thank Dr Junying Jia, Department of Pathology, University of Birmingham, for providing the EBV positive cell line (Namalwa), and Dr John Nicholas, Department of Oncology, Johns Hopkins University School of Medicine, for providing the pRPMS4.4 plasmid containing the HHV6 gene polymerase.

References

Arena, A., Liberto, M.C., Iannello, D., Capozza, A.B. & Foca, A. (1999) Altered cytokine production after human herpes virus type 6 infection. *New Microbiologica*, **22,** 293–300.

Arena, A., Iannello, D., Gazzara, D., Speranza, A., Bonina, L. & Mastroeni, P. (2001) Role of interleukin-18 in peripheral blood mononuclear cells infected with human herpes virus type 6. *Intervirology*, **44,** 250–254.

Attygalle, A., Al Jehani, R., Diss, T.C., Munson, P., Liu, H., Du, M.Q., Isaacson, P.G. & Dogan, A. (2002) Neoplastic T cells in angioimmunoblastic T-cell lymphoma express CD10. *Blood*, **99,** 627–633.

Attygalle, A., Kyriakou, C., Dupuis, J., Grogg, K.L., Diss, T.C., Wotherspoon, A.C., Chuang, S.S., Cabecadas, J., Isaacson, P.G., Du, M.Q., Gaulard, P. & Dogan, A. (2007a) Histologic evolution of angioimmunoblastic T-cell lymphoma in consecutive biopsies:

© 2007 The Authors
Journal Compilation © 2007 Blackwell Publishing Ltd,

insights into natural history and disease progression. *American Journal of Surgical Pathology*, (in press).

Attygalle, A.D., Chuang, S.S., Diss, T.C., Du, M.Q., Isaacson, P.G. & Dogan, A. (2007b) Distinguishing angioimmunoblastic T-cell lymphoma from peripheral T-cell lymphoma, unspecified, using morphology, immunophenotype and molecular genetics. *Histopathology*, **50,** 498–508.

Battegay, M., Berger, C., Rochlitz, C., Hurwitz, N., Hirsch, H.H., De Geyter, C., Haque, T. & Nadal, D. (2004) Epstein–Barr virus load correlating with clinical manifestation and treatment response in a patient with angioimmunoblastic T-cell lymphoma. *Antiviral Therapy*, **9,** 453–459.

Chadburn, A., Cesarman, E., Nador, R.G., Liu, Y.F. & Knowles, D.M. (1997) Kaposi's sarcoma-associated herpesvirus sequences in benign lymphoid proliferations not associated with human immunodeficiency virus. *Cancer*, **80,** 788–797.

Di Luca, D., Dolcetti, R., Mirandola, P., De Re, V., Secchiero, P., Carbone, A., Boiocchi, M. & Cassai, E. (1994) Human herpesvirus 6: a survey of presence and variant distribution in normal peripheral lymphocytes and lymphoproliferative disorders. *Journal of Infectious Disease*, **170,** 211–215.

Diss, T.C., Peng, H., Wotherspoon, A.C., Isaacson, P.G. & Pan, L. (1993) Detection of monoclonality in low-grade B-cell lymphomas using the polymerase chain reaction is dependent on primer selection and lymphoma type. *Journal of Pathology*, **169,** 291–295.

Diss, T.C., Watts, M., Pan, L., Linch, D. & Isaacson, P.G. (1995) The polymerase chain reaction in the demonstration of monoclonality in T cell lymphomas. *Journal of Clinical Pathology*, **48,** 1045–1050.

Dogan, A., Attygalle, A.D. & Kyriakou, C. (2003) Angioimmunoblastic T-cell lymphoma. *British Journal of Haematology*, **121,** 681–691.

Dogan, A., Ngu, L.S., Ng, S.H. & Cervi, P.L. (2005) Pathology and clinical features of angioimmunoblastic T-cell lymphoma after successful treatment with thalidomide. *Leukaemia*, **19,** 873–875.

Dukers, D.F., Jaspars, L.H., Vos, W., Oudejans, J.J., Hayes, D., Cillessen, S., Middeldorp, J.M. & Meijer, C.J. (2000) Quantitative immunohistochemical analysis of cytokine profiles in Epstein–Barr virus-positive and -negative cases of Hodgkin's disease. *Journal of Pathology*, **190,** 143–149.

Flamand, L., Gosselin, J., Stefanescu, I., Ablashi, D. & Menezes, J. (1995) Immunosuppressive effect of human herpesvirus 6 on T-cell functions: suppression of interleukin-2 synthesis and cell proliferation. *Blood*, **85,** 1263–1271.

Ganesan, T.S., Dhaliwal, H.S., Dorreen, M.S., Stansfeld, A.G., Habeshaw, J.A. & Lister, T.A. (1987) Angio-immunoblastic lymphadenopathy: a clinical, immunological and molecular study. *British Journal of Cancer*, **55,** 437–442.

Gobbi, A., Stoddart, C.A., Malnati, M.S., Locatelli, G., Santoro, F., Abbey, N.W., Bare, C., Linquist-Stepps, V., Moreno, M.B., Herndier, B.G., Lusso, P. & McCune, J.M. (1999) Human herpesvirus 6 (HHV-6) causes severe thymocyte depletion in SCID-hu Thy/Liv mice. *Journal of Experimental Medicine*, **189,** 1953–1960.

Gosselin, J., Flamand, L., D'Addario, M., Hiscott, J., Stefanescu, I., Ablashi, D.V., Gallo, R.C. & Menezes, J. (1992) Modulatory effects of Epstein–Barr, herpes simplex, and human herpes-6 viral infections and coinfections on cytokine synthesis. A comparative study. *Journal of Immunology*, **149,** 181–187.

Grogg, K.L., Attygalle, A.D., Macon, W.R., Remstein, E.D., Kurtin, P.J. & Dogan, A. (2005) Angioimmunoblastic T-cell lymphoma: a neoplasm of germinal-center T-helper cells? *Blood*, **106,** 1501–1502.

Hussell, T., Isaacson, P.G., Crabtree, J.E. & Spencer, J. (1996) *Helicobacter pylori*-specific tumour-infiltrating T cells provide contact dependent help for the growth of malignant B cells in low-grade gastric lymphoma of mucosa-associated lymphoid tissue. *Journal of Pathology*, **178,** 122–127.

Isegawa, Y., Ping, Z., Nakano, K., Sugimoto, N. & Yamanishi, K. (1998) Human herpesvirus 6 open reading frame U12 encodes a functional beta-chemokine receptor. *Journal of Virology*, **72,** 6104–6112.

Khan, G., Norton, A.J. & Slavin, G. (1993) Epstein–Barr virus in angioimmunoblastic T-cell lymphomas. *Histopathology*, **22,** 145–149.

Klein, S.C., Kube, D., Abts, H., Diehl, V. & Tesch, H. (1996) Promotion of IL8, IL10, TNF alpha and TNF beta production by EBV infection. *Leukaemia Research*, **20,** 633–636.

Kuppers, R. (2003) B cells under influence: transformation of B cells by Epstein–Barr virus. *Nature Review Immunology*, **3,** 801–812.

Luppi, M., Marasca, R., Barozzi, P., Artusi, T. & Torelli, G. (1993) Frequent detection of human herpesvirus-6 sequences by polymerase chain reaction in paraffin-embedded lymph nodes from patients with angioimmunoblastic lymphadenopathy and angioimmunoblastic lymphadenopathy-like lymphoma. *Leukaemia Research*, **17,** 1003–1011.

Luppi, M., Barozzi, P., Maiorana, A., Artusi, T., Trovato, R., Marasca, R., Savarino, M., Ceccherini-Nelli, L. & Torelli, G. (1996) Human herpesvirus-8 DNA sequences in human immunodeficiency virus-negative angioimmunoblastic lymphadenopathy and benign lymphadenopathy with giant germinal center hyperplasia and increased vascularity. *Blood*, **87,** 3903–3909.

Luppi, M., Barozzi, P., Garber, R., Maiorana, A., Bonacorsi, G., Artusi, T., Trovato, R., Marasca, R. & Torelli, G. (1998) Expression of human herpesvirus-6 antigens in benign and malignant lymphoproliferative diseases. *American Journal of Pathology*, **153,** 815–823.

Maric, I., Bryant, R., Abu-Asab, M., Cohen, J.I., Vivero, A., Jaffe, E.S., Raffeld, M., Tsokos, M., Banks, P.M. & Pittaluga, S. (2004) Human herpesvirus-6-associated acute lymphadenitis in immunocompetent adults. *Modern Pathology*, **17,** 1427–1433.

Moore, K.W., Vieira, P., Fiorentino, D.F., Trounstine, M.L., Khan, T.A. & Mosmann, T.R. (1990) Homology of cytokine synthesis inhibitory factor (IL-10) to the Epstein–Barr virus gene BCRFI. *Science*, **248,** 1230–1234.

Pan, L.X., Ramani, P., Diss, T.C., Liang, J.N. & Isaacson, P.G. (1995) Epstein–Barr virus associated lymphoproliferative disorder with fatal involvement of the gastrointestinal tract in an infant. *Journal of Clinical Pathology*, **48,** 390–392.

Pizzolo, G., Chilosi, M., Fiore-Donati, L. & Perona, G. (1983) Imbalance of peripheral blood and lymph node T cell subpopulations in angioimmunoblastic lymphadenopathy. Report of three cases. *Haematologica*, **68,** 591–599.

Ree, H.J., Kadin, M.E., Kikuchi, M., Ko, Y.H., Go, J.H., Suzumiya, J. & Kim, D.S. (1998) Angioimmunoblastic lymphoma (AILD-type T-cell lymphoma) with hyperplastic germinal centers. *American Journal of Surgical Pathology*, **22,** 643–655.

Ree, H.J., Kadin, M.E., Kikuchi, M., Ko, Y.H., Suzumiya, J. & Go, J.H. (1999) Bcl-6 expression in reactive follicular hyperplasia, follicular lymphoma, and angioimmunoblastic T-cell lymphoma with hyperplastic germinal centers: heterogeneity of intrafollicular T-cells and their altered distribution in the pathogenesis of angioimmunoblastic T-cell lymphoma. *Human Pathology*, **30,** 403–411.

© 2007 The Authors

Schnitzer, B. (1995) Surgical pathology of the lymph nodes and related organs. In: *Reactive lymphoid heperplasias* (ed. by E.S. Jaffe), pp. 117–119. W.B. Saunders company, Philadelphia.

Skinnider, B.F. & Mak, T.W. (2002) The role of cytokines in classical Hodgkin lymphoma. *Blood*, **99,** 4283–4297.

Strupp, C., Aivado, M., Germing, U., Gattermann, N. & Haas, R. (2002) Angioimmunoblastic lymphadenopathy (AILD) may respond to thalidomide treatment: two case reports. *Leukaemia and Lymphoma*, **43,** 133–137.

Uchihara, J.N., Krensky, A.M., Matsuda, T., Kawakami, H., Okudaira, T., Masuda, M., Ohta, T., Takasu, N. & Mori, N. (2005) Transactivation of the CCL5/RANTES gene by Epstein–Barr virus latent membrane protein 1. *International Journal of Cancer*, **114,** 747–755.

Vrsalovic, M.M., Korac, P., Dominis, M., Ostojic, S., Mannhalter, C. & Kusec, R. (2004) T- and B-cell clonality and frequency of human herpes viruses-6, -8 and Epstein–Barr virus in angioimmunoblastic T-cell lymphoma. *Hematological Oncology*, **22,** 169–177.

Wang, L.R., Dong, L.J., Zhang, M.J. & Lu, D.P. (2006) The impact of human herpesvirus 6B reactivation on early complications following allogeneic hematopoietic stem cell transplantation. *Biology of Blood Marrow Transplantation*, **12,** 1031–1037.

Weiss, L.M., Jaffe, E.S., Liu, X.F., Chen, Y.Y., Shibata, D. & Medeiros, L.J. (1992) Detection and localization of Epstein–Barr viral genomes in angioimmunoblastic lymphadenopathy and angioimmunoblastic lymphadenopathy-like lymphoma. *Blood*, **79,** 1789–1795.

Willenbrock, K., Renne, C., Gaulard, P. & Hansmann, M.L. (2005) In angioimmunoblastic T-cell lymphoma, neoplastic T cells may be a minor cell population. A molecular single-cell and immunohistochemical study. *Virchows Archiv*, **446,** 15–20.

Wotherspoon, A.C. (1997) Gastric MALT lymphoma and *Helicobacter pylori*. *Yale Journal of Biology and Medicine*, **69,** 61–68.

Yasukawa, M., Inoue, Y., Ohminami, H., Terada, K. & Fujita, S. (1998) Apoptosis of CD4+ T lymphocytes in human herpesvirus-6 infection. *Journal of General Virology*, **79,** 143–147.

Zou, P., Isegawa, Y., Nakano, K., Haque, M., Horiguchi, Y. & Yamanishi, K. (1999) Human herpesvirus 6 open reading frame U83 encodes a functional chemokine. *Journal of Virology*, **73,** 5926–5933.

© 2007 The Authors
Journal Compilation © 2007 Blackwell Publishing Ltd,